Equatorial bubbles as observed with GPS measurements over Pune, India

A. DasGupta,[1,2] A. Paul,[2] S. Ray,[1] A. Das,[1] and S. Ananthakrishnan[3]

Received 31 August 2005; revised 22 February 2006; accepted 1 March 2006; published 8 June 2006.

[1] Ionospheric total electron content (TEC) and scintillations have been recorded continuously since April 2003 using a dual-frequency GPS receiver at Pune, India (geographic latitude 19.1°N, longitude 74.05°E; 24°N dip), situated in between the magnetic equator and the northern crest of the equatorial anomaly. The TEC often shows bite-outs when severe amplitude scintillations are observed on the GPS L1 carrier level. The apparent duration of the bite-outs may be different from the true east-west duration, as observed with geostationary links, because of the presence of a relative velocity between the irregularity cloud and the satellite. The trajectory of a GPS satellite plays an important role in observing the bubble characteristics. The distributions of amplitude and duration of the bubbles have been obtained during the equinoctial months February through April of 2004. The median values are found to be 9 TEC units (1 TECU = 10^{16} el/m^2) and 3.3 min, respectively. The range error at GPS L1 frequency corresponding to the median TEC depletion is 1.4 m, while that corresponding to the 95th percentile value is 4.5 m. An asymmetry in the east-west walls of the bubble and sharp edges of the depletions resulting in high range error rates ~30 cm/min has been noted.

Citation: DasGupta, A., A. Paul, S. Ray, A. Das, and S. Ananthakrishnan (2006), Equatorial bubbles as observed with GPS measurements over Pune, India, *Radio Sci.*, *41*, RS5S28, doi:10.1029/2005RS003359.

1. Introduction

[2] The irregularities in the *F* region of the ionosphere in the equatorial region occur in the form of depletions, frequently referred to as "bubbles." Excellent review articles on equatorial ionospheric *F* region irregularities are available [*Fejer and Kelley*, 1980; *Basu and Basu*, 1985]. The depletions that originate over the magnetic equator in the postsunset hours extend in both horizontal and vertical directions. The bubbles are upwelled by electrodynamic $\mathbf{E} \times \mathbf{B}$ drift over the magnetic equator and map down to off-equatorial locations along magnetic field lines in the form of "bananas." These bubbles may sometimes rise to great heights, exceeding 1000 km above the magnetic equator. Radar maps show that the irregularities extend in the east-west direction over several hundred kilometers near the magnetic equator [*Woodman and La Hoz*, 1976; *Kelley*, 1989; *Tsunoda et al.*, 1982]. The total electron content (TEC) of the ionosphere is mainly weighted by the ionization near the maximum of the *F* layer and topside. The depletions extending over several hundred kilometers in the topside will thus have signatures on the TEC.

[3] The effects of ionization depletions on the Faraday rotation records of geostationary satellites have been used along with amplitude scintillations to study the characteristics, namely, the amplitude and east-west extent of the equatorial bubbles [*Yeh et al.*, 1979]. Occurrences and behavior of 137 MHz VHF amplitude scintillations and associated ionospheric electron content depletions observed at Arequipa, Peru (geographic latitude 16.4°S, longitude 71.5°W; magnetic dip 9°S), during the solar maximum 1979–1980 have been studied [*DasGupta et al.*, 1983]. *Abdu et al.* [1985] reported examples of TEC depletions and associated irregularities in Faraday rotation angle (representative of the TEC of the ionosphere) on a VHF beacon at 136 MHz from a geostationary satellite recorded at equatorial and low-latitude stations. The bubbles were found to have steep walls on the leading and trailing

[1] S. K. Mitra Center for Research in Space Environment, University of Calcutta, Calcutta, India.
[2] Institute of Radio Physics and Electronics, University of Calcutta, Calcutta, India.
[3] Tata Institute of Fundamental Research, National Center for Radio Astrophysics, Pune, India.

0048-6604/06/2005RS003359

edges evident from the large time rate of change of the Faraday rotation angle. Airglow observations with all-sky cameras establish that the irregularity clouds become narrower with latitude on both sides of the magnetic equator [*Weber et al.*, 1980]. With the help of orbiting satellites, it has been found that the equatorial irregularity belt extends to about ±35° dip [*Sinclair and Kelleher*, 1969]. Both airglow observations and scintillations with orbiting satellites show that the irregularity clouds may split into several streams as one moves away from the equator [*Bhar et al.*, 1970].

[4] Effects of scintillations on GPS-based navigation and communication systems have been extensively studied [*Bandyopadhyay et al.*, 1997; *Kintner et al.*, 2001, 2004; *DasGupta et al.*, 2004a; *Rodrigues et al.*, 2004]. Recently, scintillations of GPS satellite L1 signal have been used to study the latitudinal extent of the irregularity belt [*DasGupta et al.*, 2004b]. The bubbles normally drift from west to east. As a bubble moves across a satellite link, ionization depletions and scintillations are usually encountered. The parameters characterizing the ionization depletions, namely, the depth, duration, and leading and trailing edge slopes, provide valuable information to system designers. An estimate of the range error, extent of the bubble, and ionization gradients measured in the equatorial region provides an indication for possible GPS system outages.

[5] The time rate of change of TEC and its standard deviation measured using GPS transmissions at Ascension Island (geographic latitude 7.95°S, longitude 14.41°W; magnetic latitude 16°S) have been shown to be indicators of the presence of scintillation-causing irregularities [*Basu et al.*, 1999]. GPS TEC and carrier phase measurements also show equatorial depletions. Since the GPS satellites apparently have a slow motion, the observed effect will be due to a combination of several factors. In order to study the characteristics of bubbles, the geometry of the GPS links with respect to the field-aligned bubbles has to be considered.

[6] When a bubble drifting eastward crosses a geostationary satellite link, the east-west extent of the observed ionization depletions are determined solely by the irregularity drift. Duration of bubbles observed with GPS transmissions, where the satellites are slowly moving, is dependent on the relative motion of the satellite at the pierce point altitude and the drift of the ionospheric irregularities. The orientation of the satellite trajectory also plays an important role in determining whether a component of its velocity will be parallel or antiparallel to the irregularity drift. If the satellite track velocity has an eastward component, the duration of the observed bubble will be prolonged as the irregularities normally move from west to east. In such cases, the fading rate of the scintillation patch may become very slow and may adversely affect the GPS receiver's tracking performance, leading to GPS L1 and L2 cycle slips [*Kintner et al.*, 2001]. On the other hand, if the satellite pierce point track velocity is westward, the duration of the observed bubble will be reduced. In addition, since the GPS orbit has an inclination of 55°, the actual east-west horizontal duration may be obtained from the observed duration using the geometrical secant factor of the orbital inclination projected at the ionospheric pierce point altitude. Observation of bubbles using GPS transmissions thus requires a very careful analysis. This paper critically examines the influence of the GPS trajectory on the observed features of the bubble and presents a study on the characteristics of the bubbles observed with GPS satellites from a station situated in between the magnetic equator and the northern crest of the equatorial ionization anomaly in the Indian longitude sector.

2. Data

[7] A dual-frequency semicodeless (Allen Osborne) GPS receiver has been in operation at the Giant Meterwave Radio Telescope (GMRT) (geographic latitude 19.1°N, longitude 74.05°E; dip 24°N) site near Pune since April 2003. This paper is based on GPS total electron content (TEC) measured from group delay (TECtau) and the signal-to-noise ratio (SNR-CA) at L1 frequency when the receiver is operated in the coarse acquisition (C/A) mode at a sampling frequency of 1 Hz during the equinoctial months, February through April, of 2004. The sunspot number during this period varied from 13 to 88.

[8] A location like GMRT situated in between the magnetic equator and the northern crest of the equatorial ionization anomaly is ideally suited for studying the equatorial bubbles. GPS links toward the north of the station normally look through the northern crest of the equatorial anomaly and would frequently encounter the northern limit of the equatorial irregularity belt. Looking toward the south, an end-on view of field-aligned bubbles over a longer path can be possible in the satellite-to-ground propagation path. Normally, north-south satellite trajectories showing scintillations over a long period with transition from intense scintillations to no scintillations or vice versa correspond to crossing over the northern edge of the irregularity cloud. In order to determine the east-west dimension of the bubbles moving across the line of sight, these two extreme situations have to be avoided. GPS transits exhibiting clear edges of scintillations on SNR records and associated depletions, which are observed to cross a particular link within a cone of 30° around the zenith (i.e., above 60° elevation), are selected. The TEC data are subject to a 90-min moving average and are referred to as TEC-mov-avg. Deviations

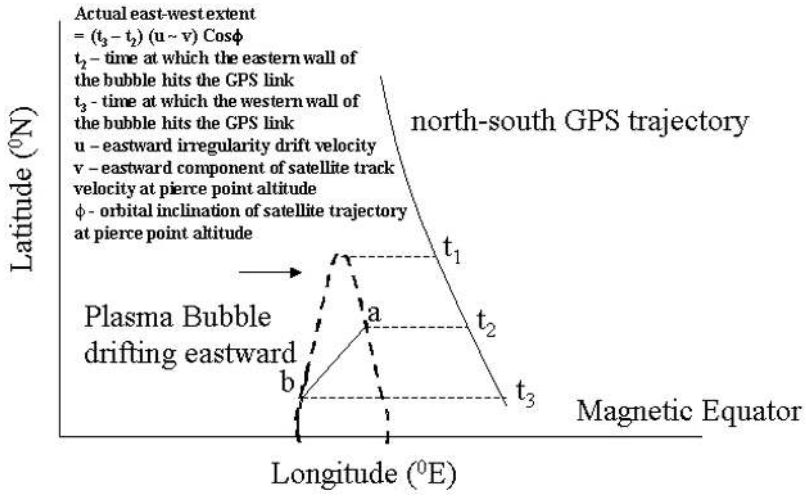

Figure 1. Sketch of a typical equatorial plasma bubble, which is wide over the magnetic equator and narrows down north of the station, drifting eastward. A north-south GPS trajectory is intercepted by the bubble during the time interval ($t_3 - t_2$), where t_2 corresponds to the time when the eastern wall of the bubble hits the GPS link, and t_3 corresponds to the time when the western wall hits the link. Section *ab* is the apparent spatial extent of the bubble.

from the average value are used for measuring the amplitude and duration of a bubble.

3. Results

[9] The spatial variation of a typical bubble and the GPS link positions with time is sketched in Figure 1. The bubble is wide over the magnetic equator and gradually tapers down at higher latitudes. The bubble, which drifts eastward, may be developed at the meridian of the station or west of it. A representative GPS trajectory from north to south at the ionospheric pierce point height is also drawn. At time t_1, the GPS satellite may be at the latitude corresponding to the northern limit of the feet of the equatorial irregularity. However, no scintillation patches on signal-to-noise ratio (SNR) records or depletions in the total electron content (TEC) would be noted at this time, as the bubble does not intersect the satellite trajectory. Because of simultaneous movements of the link and the bubble, at time t_2, when the eastern edge of the plasma bubble corresponding to point *a* first hits the GPS satellite link, fluctuations will start on the SNR coupled with the leading edge of the TEC depletion. At a later time t_3, the western wall of the irregularity corresponding to point *b* crosses the GPS trajectory. Fluctuations in SNR will die down, and the trailing edge of the depletion will be observed. Thereafter, the bubble drifting eastward does not intercept this GPS satellite trajectory anymore. Thus the scintillation patch observed by the GPS link would have duration of ($t_3 - t_2$). In calculating the actual east-west horizontal extent, the relative motion between the irregularity and the satellite at the ionospheric pierce point height has to be taken into account. Irregularities normally move from west to east with an average velocity of 100 m/s [*Fejer et al.*, 1985]. Thus, if the satellite is moving eastward, the apparent duration of the bubble would be longer. On the other hand, if the satellite moves westward, the observed duration would be diminished. In other words, the vector sum of the ionospheric projection of the satellite velocity and the irregularity drift orthogonal to the propagation path determines the spatial extent of the irregularity bubble [*Basu et al.*, 1999]. During the interval ($t_3 - t_2$), the eastward drift velocity of the plasma bubble is parallel to the eastward component of the pierce point projected satellite track velocity. In the present case, the duration of the observed bubble would be prolonged by the combination of these two velocities. The section marked *ab* would give an apparent east-west extent of the bubble. Since the GPS orbit has an inclination of 55°, the actual east-west dimension may be obtained by dividing the observed extent with the geometrical secant factor (orbital inclination projected at the ionospheric pierce point altitude). For a satellite trajectory moving from south to north, the sequence of events would be reversed.

[10] Figure 2 shows a typical sample of signal-to-noise ratio of the satellite link (SNR-CA), operated in the coarse acquisition (C/A) mode, showing intense scintillations and associated depletions in TEC calculated from group delay (TECtau) of GPS satellite SV25 on 25 March 2004. The 90-min moving average of TECtau (TEC-mov-

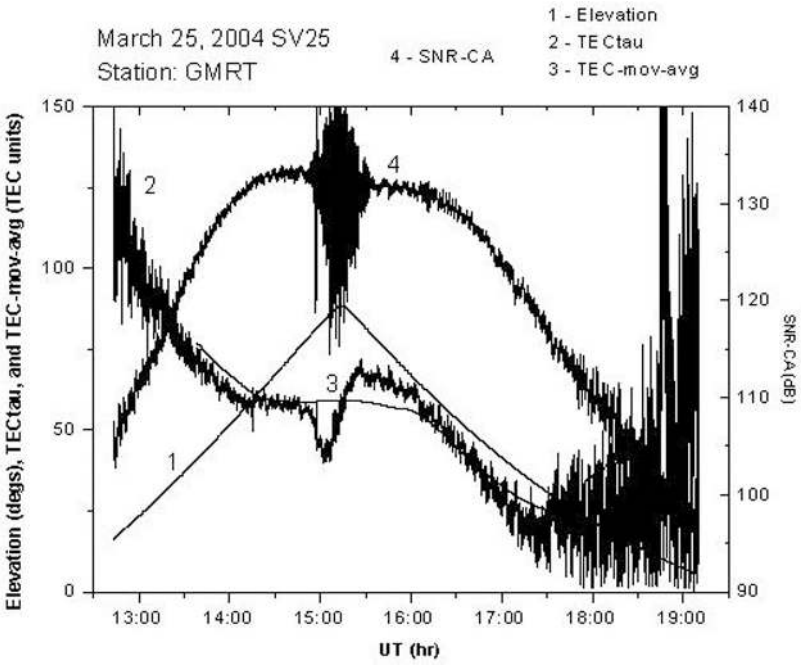

Figure 2. Typical sample record from GPS satellite SV25 observed from the GMRT site on 25 March 2004. Curve 1 refers to the elevation angle of the satellite during its transit, curve 2 represents the total electron content (TEC) calculated from the group delay (TECtau), curve 3 is the 90-min moving-averaged TECtau (TEC-mov-avg), and curve 4 shows the signal-to-noise ratio for the satellite link operated in the coarse acquisition (C/A) mode (SNR-CA).

avg) is shown along with TECtau. Large fluctuations in TECtau near the ends of the track could be ascribed to multipath effects at low elevation angles. The TEC depletion, which occurred from 1448–1518 UT, had amplitude of 19 TEC units (1 TECU = 10^{16} el/m^2) over an ambient of 59 TECU. The 350-km subionospheric points corresponding to the depletion were (18.40°N, 73.84°E) and (19.21°N, 73.99°E). The SNR-CA records were clear prior to and after the bubble. The eastern wall of the depletion is found to have a slope of 1.08 TECU/min, while the western wall has a slope of 1.2 TECU/min.

[11] Figure 3 shows the trajectories of GPS satellites SV13, 20, and 25 at the ionospheric height of 350 km tracked from the GMRT site during the night of 25 March 2004. The starting and ending times of the tracks are also marked in Figure 3. During 1200–2400 UT (1800–0600 LT), 17 GPS satellites, namely, SV1, 3, 7, 8, 11, 13, 14, 15, 16, 18, 20, 21, 22, 25, 27, 28, and 30 were tracked. A typical sketch of an equatorial bubble, which is wide over the magnetic equator and narrows down to the north of the station, is again shown. The smaller ellipse around the station indicates the zone of reception with 60° elevation mask. The bigger ellipse is the zone of reception from the GMRT site with 5° elevation mask. The magnetic equator and the northern crest of the equatorial anomaly around 30°N dip are also shown in Figure 3. GPS satellite SV25, which shows fluctuations in SNR and an associated bite-out in TEC around 1500 UT (Figure 2), moves from south-west to north-east nearly along a meridian during the interval 1415–1615 UT. From 1815 UT onward until the end of the track at 1911 UT, it moved in an eastward direction with practically no north-south motion. In the absence of an irregularity, the SNR showed a clean record. An irregularity drifting from west to east crossed the track of SV25 around 1500 UT, triggering fluctuations in SNR and bite-outs in TEC. Thereafter, the satellite link moving in an eastward direction crossed the eastern wall of the irregularity.

[12] This transition from a no-scintillation zone north of the present station to the equatorial belt could be understood from a more or less north-south GPS trajectory. Figure 4 shows the plot of signal-to-noise ratio (SNR-CA) of GPS SV15 recorded from the GMRT site on 8 March 2004 during 1230–1730 UT. The 350-km subionospheric track of SV15 is shown in the inset. SV15 moved from north of the station southward. Fluctuations in SNR-CA started around 1430 UT when the pierce point of the satellite was north of the station at

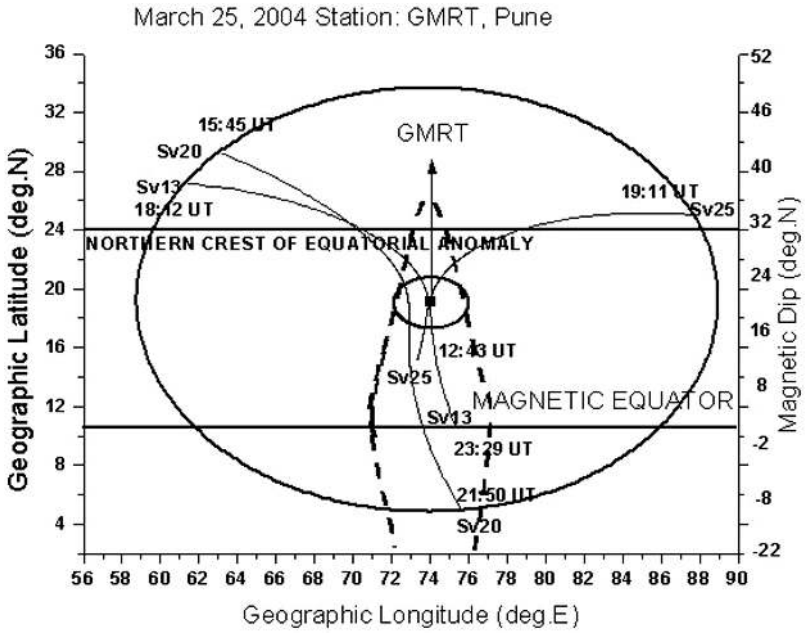

Figure 3. Tracks of GPS satellites SV13, 20, and 25 at the ionospheric height of 350 km observed from the GMRT site on 25 March 2004 over the time interval 1200–0000 UT (1800–0600 LT). The small ellipse around the station indicates the zone of reception above the 60° elevation mask, while the bigger ellipse is the zone of reception from the GMRT site with 5° elevation mask. The sketch of a typical equatorial bubble, drifting eastward, which is wide over the magnetic equator and narrows down to the north of the station, is shown by the dotted curve. The magnetic equator and the northern crest of the equatorial anomaly around the 30° dip are also shown.

19.3°N and continued until 1700 UT, when the subionospheric location of the satellite was at 11.4°N. The presence of a clear record prior to onset of fluctuations in SNR-CA indicates the possibility of the satellite link crossing the northern limit of the equatorial irregularity belt around 1430 UT. Scintillations in excess of 10 dB were observed from 1430 to 1700 UT, a period of 150 min. Assuming an average east-west drift velocity of 100 m/s, this corresponds to an east-west extent of 900 km. Although it is not impossible to have a 900-km-wide irregularity cloud, it is unlikely to be observed frequently from a station like GMRT situated away from the magnetic equator. Furthermore, a 900-km east-west wide irregularity patch is likely to simultaneously include other GPS links also. A north-south moving satellite in the Northern Hemisphere sometimes shows scintillations over a prolonged period with clean records on the north. These satellites may also sometimes view the field-aligned ''bubbles'' end on over a longer path when they move south over the magnetic equator and may exhibit enhanced scintillations. Figure 5 illustrates this transition from the intense equatorial belt to the no-scintillation midlatitude region as seen from Calcutta (geographic latitude 22.58°N, longitude 88.38°E; dip 32°N), situated at latitude higher than that of GMRT. This feature is regularly observed from Calcutta, which is situated near the northern crest of the equatorial anomaly in the Indian longitude zone.

[13] The subionospheric trajectories of GPS satellites play an important role as far as observing bubbles are concerned. The distances of different satellites' 350-km pierce point longitudes from the GMRT meridian (74.05°E) explain this point. These distances may be calculated from the differences of the satellite's pierce point longitude from the GMRT meridian. If an eastward location of the pierce point with respect to the station meridian is taken as positive and a westward location as negative, satellites with a prolonged constant positive distance from the meridian would understandably be moving in a north-south direction along a meridian east of GMRT with very little west-east motion during the above time interval. Duration of bubbles observed by such satellite trajectories would then be unaffected by any eastward/westward component of satellite velocity and would mainly be determined by the eastward drift of the bubble. On the other hand, satellite trajectories having an inclined orientation would be moving either toward or away from the GMRT meridian with a

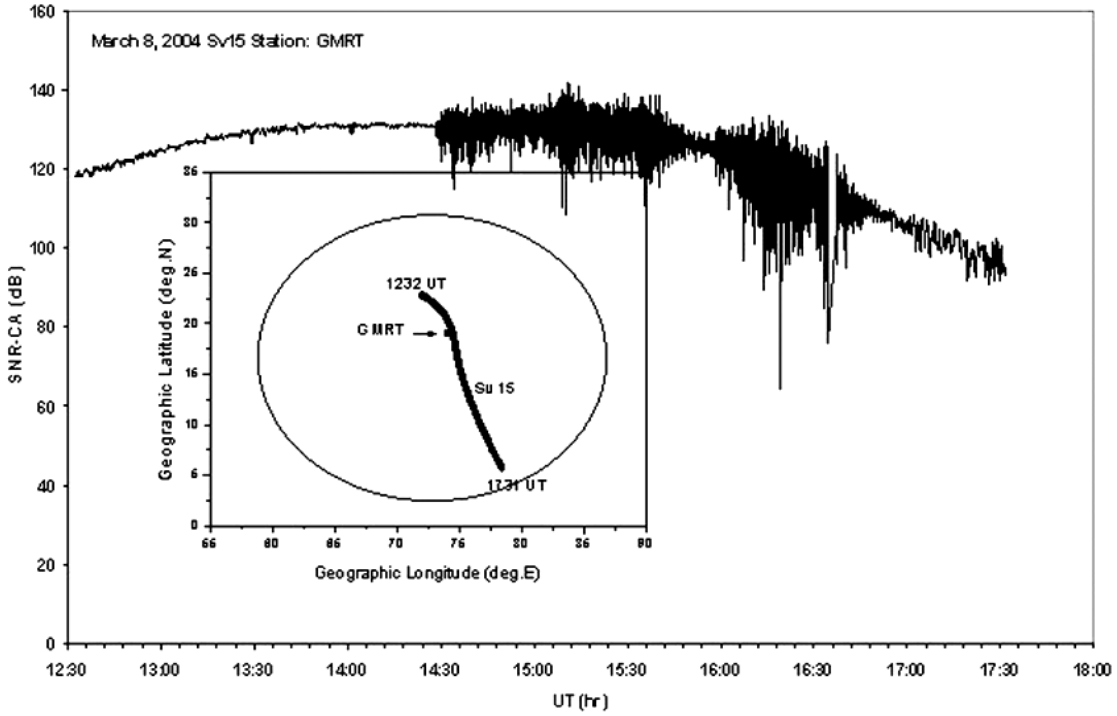

Figure 4. SNR-CA for SV15 plotted against universal time observed from the GMRT site on 8 March 2004. The inset shows the track of the same satellite with the start and end time. The ellipse indicates the zone of reception at 5° mask angle.

pronounced eastward/westward component of velocity at the pierce point.

[14] An idea about the eastward/westward component of the ionospheric pierce point projected GPS satellite track velocity can be obtained from Figure 6, which shows the same for 25 March 2004 from the GMRT site during 1300–0030 UT (1900–0630 LT). Satellite tracks, with a progressively increasing positive distance or a progressively decreasing negative distance from the GMRT meridian, have positive eastward velocities. Satellites SV13, 20, and 25 are labeled, and portions of their tracks, which exhibited TEC depletions in excess of 1 TECU above an elevation of 60°, are indicated by thick lines. Satellite SV25 was initially at a western location with respect to GMRT. It moved eastward toward the station meridian and beyond with a progressively increasing positive distance and had a positive eastward component of velocity throughout its track. Satellites SV13 and 20 were initially at a far-west longitude from the station meridian on 25 March 2004. They moved eastward toward the station meridian with progressively decreasing negative distance, crossed the station meridian, and moved further eastward with progressively increasing positive distance. As a result, their 350-km projected track velocities were always eastward. The striking feature of Figure 6 is the concentration of the eastward component of the pierce point projected satellite velocities around 100–150 m/s, particularly during 1630–2030 UT on 25 March 2004. This suggests that the apparent duration of bubbles would be more than the actual duration. When the eastward component of velocity of the ionospheric intersection point of a GPS satellite becomes 100–150 m/s and nearly matches the eastward velocity of a bubble, the fading rate may become very slow. This may adversely affect the GPS receiver's tracking performance when the depth of fading or scintillations is strong and results in GPS L1 and L2 cycle slips [*Kintner et al.*, 2001].

[15] Figure 7 shows the distribution of the TEC depletions in equatorial plasma bubbles observed from the GMRT site within the selected elevation swath (greater than 60°) during February through April 2004. It may be noted that out of the observed 45 bite-outs, the maximum amplitude was found to be about 33 TECU over an ambient of 40 TECU and a median depletion of about 9 TECU against an ambient 33 TECU. The maximum amplitude corresponds to a range error of about 5.3 m at GPS L1 frequency and the median to about 1.4 m

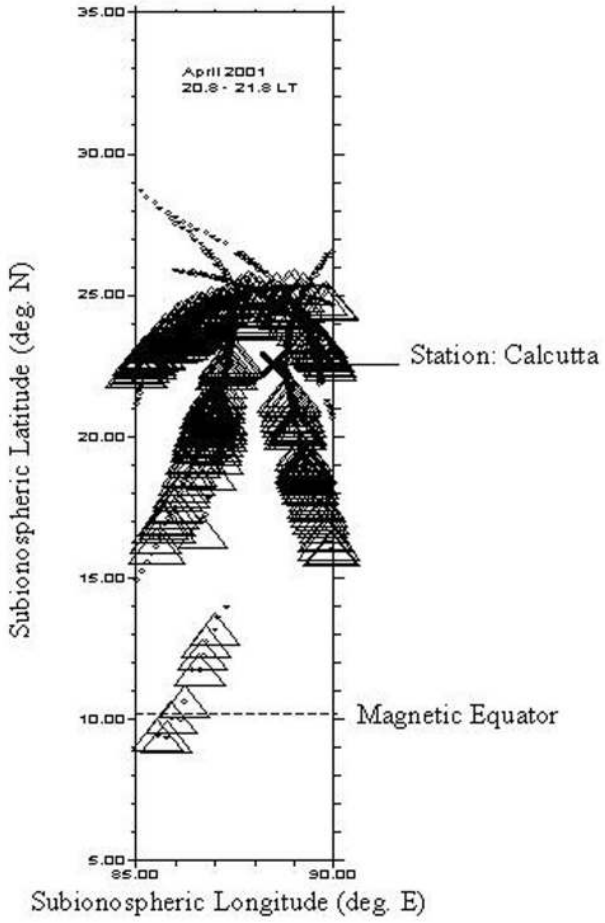

Figure 5. Plot of 350-km subionospheric tracks of GPS satellites observed from Calcutta during 2048–2148 LT in April 2001. The triangles represent points on the track with scintillations in excess of 15 dB, and the dots represent points with no scintillations. The position of the station is indicated by the cross. Observations had been limited to a 5° longitude swath about the station. The traces are smudged because of overlapping of several GPS passes observed over 1 month.

range error. The ambient range error in the equatorial region may be much more than this value. But its variation is smooth in nature, whereas the bubbles introduce a relatively sharper change.

[16] Figure 8a shows the distribution of the duration of bubbles. Taking the geometry of the GPS trajectory into account, that is, the projected inclination of GPS satellites' trajectories at 350 km ionospheric height, the converted duration corresponding to the east-west dimension is shown in Figure 8b. The majority of the bubbles have duration less than 5 min with a maximum of 14 min. Assuming an average eastward irregularity drift velocity of 100 m/s, the maximum corresponds to an extent of about 80 km and the median 30 km.

[17] The observed bubbles often show asymmetry between the leading (eastern) and trailing (western) edges. Figures 9a and 9b compare the slopes of eastern and western walls of the bubbles. It may be noted that in general, the trailing slope, that is, the western wall, is sharper than the leading slope, that is, the eastern wall. The leading edge slope has a maximum value of 3 TECU/min with a median of about 1 TECU/min. While the maximum corresponds to a range error rate of 48 cm/min, the median yields a range error rate of 16 cm/min. The noted maximum value of the trailing edge slope of 14.4 TECU/min and median of 1.8 TECU/min in Figure 9b conform to the idea of asymmetric edges of the bubble. In this case, the maximum value produces a range error rate of 2.3 m/min and the median 29 cm/min.

4. Discussion

[18] This paper critically discusses the problems associated with observations of equatorial bubbles by using GPS transmissions. As the bubbles extend several hundred kilometers on the topside, their characteristics could be studied from depletions in the ionospheric total electron content (TEC), which gives a height-integrated profile of ionization. Selection of GPS links plays an important role in the observed features. The statistics of equatorial plasma bubbles calculated from depletions in TEC in the local postsunset hours around a location like the GMRT site near Pune, which is situated in between the magnetic equator and the northern crest of the equatorial anomaly in the Indian zone, are presented.

[19] The feet of the field tube actually determine the latitudinal extent of the irregularity belt. Bubbles, which are generated west of the station and extend northward from the magnetic equator, move eastward with an average velocity of about 100 m/s. A satellite link first records scintillations when it encounters an edge of the irregularity cloud. In the case of geostationary satellites, where the link is fixed in time and space, normally, the eastern edge of the irregularity hits the link first. With GPS, the first recording of scintillations will depend on the combined effect of the slowly drifting GPS track and the eastward moving irregularity. When a north-south moving GPS track encounters the northern edge and moves through an irregularity cloud, the link will normally show scintillations over a longer period of time. On the other hand, an east-west movement will result in scintillations or bubbles over a relatively shorter interval of time.

[20] The subionospheric trajectories of GPS satellites play an important role as far as observing bubbles are concerned. Duration of bubbles observed by GPS satel-

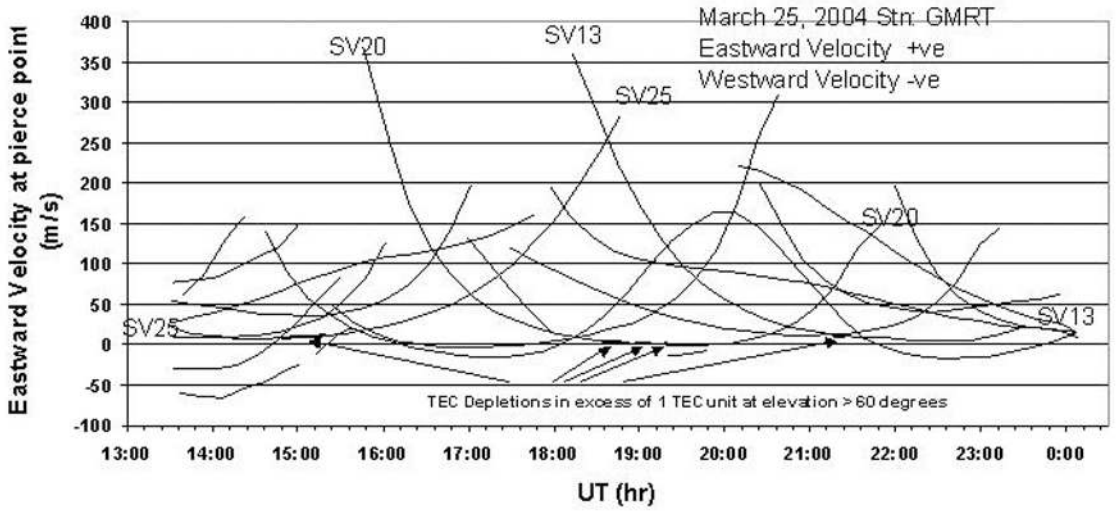

Figure 6. Velocity of different GPS satellites projected at the ionospheric height of 350 km measured from the GMRT site on 25 March 2004 during 1300–0030 UT. Positive value indicates an eastward component, while negative value indicates a westward component. GPS satellites SV13, 20, and 25 are labeled, and portions of their tracks showing TEC depletions in excess of 1 TECU above an elevation of 60° are marked by thick lines.

lites moving in a north-south direction with very little west-east motion would be unaffected by any westward/eastward component of satellite velocity and would mainly be determined by the eastward drift of the bubble. On the other hand, GPS satellites with a predominant eastward/westward velocity and very little north-south component while crossing over an irregularity cloud could be used to determine the east-west extent of the bubble by taking into account the ionospheric pierce point projected velocity of the satellite. The east-west dimension is, however, dependent on the magnetic latitude and would be wider over the magnetic equator. The actual direction of motion of the satellite, whether eastward or westward, determines whether the apparent duration of TEC bite-outs as observed along the track of a satellite would be greater or less than the actual duration.

[21] Effects of scintillations on GPS-based navigation and communication systems have been extensively addressed [*Bandyopadhyay et al.*, 1997; *Kintner et al.*, 2001, 2004; *DasGupta et al.*, 2004a]. *Bandyopadhyay et al.* [1997] reported some examples of degradation in the position accuracy during periods of scintillation activity. *DasGupta et al.* [2004a] have shown that the accuracy of position fixing with GPS is severely degraded during periods of intense scintillations in high sunspot number years near the crest of the equatorial anomaly. *Kintner et al.* [2001, 2004] had pointed out that when the ionospheric pierce point velocity of a moving receiver and the scintillation ground diffraction pattern velocity

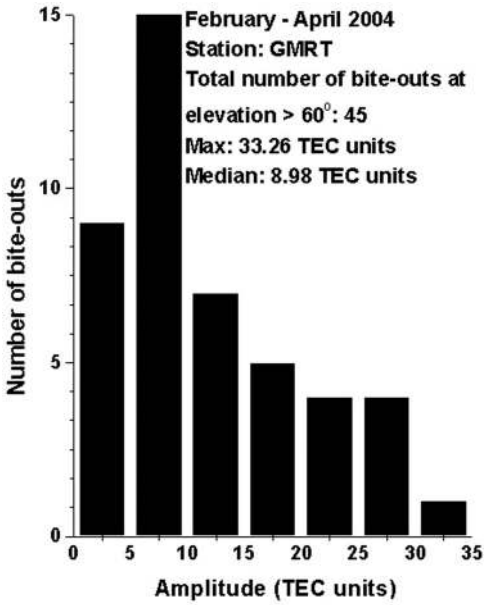

Figure 7. Amplitude distribution of TEC depletions observed from the GMRT site along the tracks of different GPS satellites during February–April 2004 at elevation angles exceeding 60°.

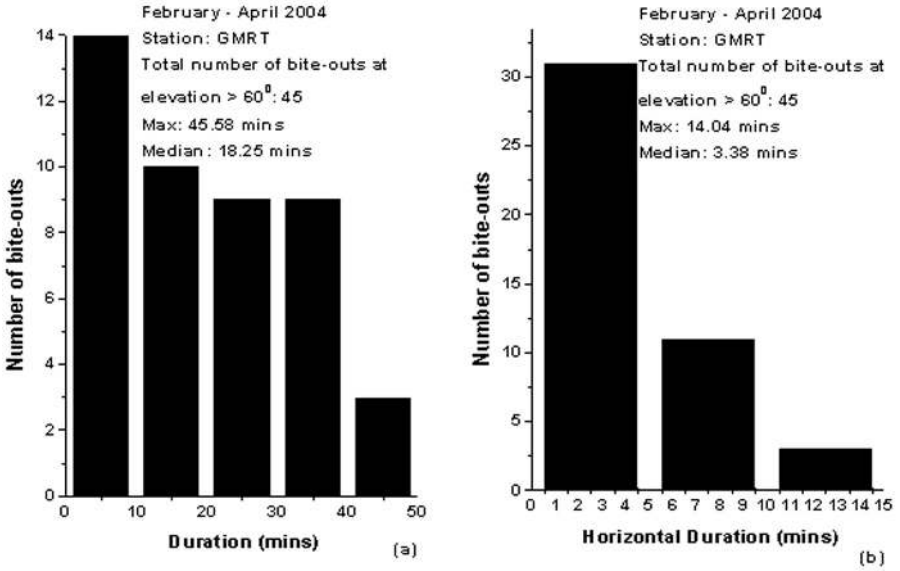

Figure 8. (a) Distribution of duration of bite-outs in TEC along the tracks of different GPS satellites observed from the GMRT site during February–April 2004 when the elevation angle is greater than 60°. (b) Distribution of west-east duration of bite-outs in TEC taking into account the projected inclination of the GPS orbits at the ionospheric height of 350 km.

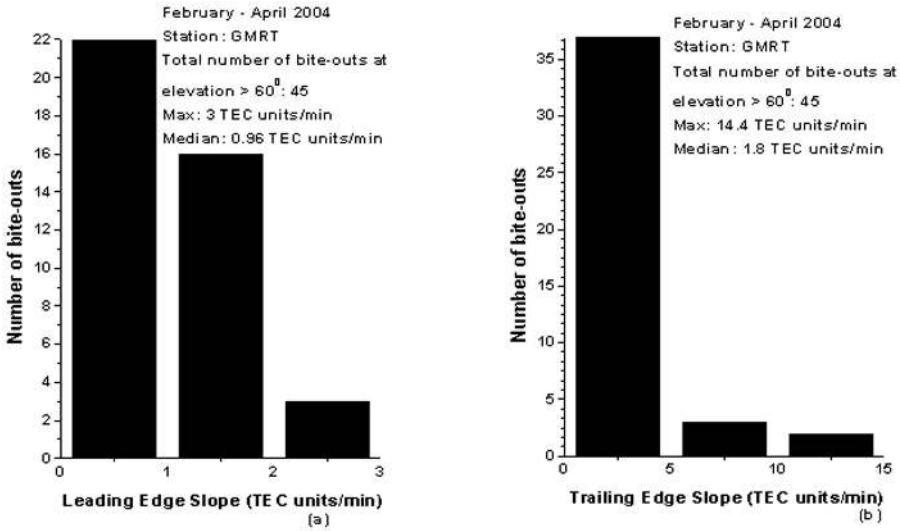

Figure 9. (a) Distribution of leading (eastern wall of the irregularity) edge of the bite-out in TEC observed from the GMRT site along the tracks of different GPS satellites during February–April 2004 at elevation angles exceeding 60°. (b) Distribution of trailing (western wall of the irregularity) edge of the bite-out in TEC observed from the GMRT site along the tracks of different GPS satellites during February–April 2004 at elevation angles exceeding 60°.

match, the probability of loss of lock increases because of the longer duration of the amplitude fades. This case of a moving GPS receiver would be applicable to receivers on board airplanes. Airborne receivers with a predominant east-west motion are more likely to resonate or match velocities with scintillation fade patterns than receivers having a north-south component of motion, where resonance will occur only for specific orientations and projection angles [*Rodrigues et al.*, 2004].

[22] The characteristics of the bubbles, namely, the amplitude and the asymmetric edges, had been studied earlier using observations from geostationary satellites [*DasGupta et al.*, 1983; *Abdu et al.*, 1985]. The depletions in TEC associated with VHF amplitude scintillations at 137 MHz recorded at Arequipa, Peru (geographic latitude 16.4°S, longitude 71.5°W; magnetic dip 9°S), during the solar maximum period 1979–1980 have been found to have a typical duration of 10–15 min and amplitude less than 5 TECU, although depletions with amplitude as large as 20 TECU and with duration of more than 30 min had sometimes been encountered [*DasGupta et al.*, 1983]. Examples of TEC depletion events registered on a 136 MHz VHF beacon recorded at equatorial and low-latitude stations in the Brazilian longitude sector during the equinoctial and local summer December–January months of 1982–1983 using the Faraday rotation technique show a steep rate of change of the order of 7°/min [*Abdu et al.*, 1985]. The sharper western wall of the irregularity measured at the GMRT site may in part be attributed to the effect of the neutral wind [*Tsunoda*, 1981]. The maximum gradient of the western wall has been found to be 14.4 TECU/min in the present case. Such steep edges of TEC depletions are quite frequent even under magnetically quiet conditions in the equatorial ionosphere, particularly during the equinoctial months of the solar maximum period. However, in the midlatitudes, enhancements with such sharp edges are usually associated with a magnetically disturbed ionosphere. During the super magnetic storm of 30 October 2003, a large storm-enhanced density (SED) plume extended over the continental United States and Canada in a southeast to northwest direction, with the largest TEC exceeding 200 TECU in the western United States. Large TEC fluctuations, on the order of 5 TECU/min, in a quasi-magnetic east-west direction along lines of geomagnetic latitude and also in a southeast to northwest direction following the large TEC gradients of the SED, were noted [*Basu et al.*, 2005]. The median value of the amplitude of TEC bite-out observed from the GMRT site, which corresponds to 1.4 m range error at GPS L1 frequency, coupled with the sharp edges of the depletions results in high range error rates ~30 cm/min, which may pose serious problems for position fixing using GPS in the equatorial region, even under magnetically quiet conditions.

[23] **Acknowledgments.** This research has been sponsored in part by the Indian Space Research Organization through the S. K. Mitra Center for Research in Space Environment, University of Calcutta. The authors thank Deepak Bhong of the Giant Meterwave Radio Telescope for looking after the experimental aspects of GPS observations. The authors are grateful to the reviewers for helpful suggestions.

References

Abdu, M. A., I. S. Batista, J. H. A. Sobral, E. R. de Paula, and I. J. Kantor (1985), Equatorial ionospheric plasma bubble irregularity occurrence and zonal velocities under quiet and disturbed conditions, from polarimeter observations, *J. Geophys. Res.*, *90*, 9921–9928.

Bandyopadhyay, T., A. Guha, A. DasGupta, P. Banerjee, and A. Bose (1997), Degradation of navigational accuracy with the Global Positioning System during periods of scintillation at equatorial latitudes, *Electron. Lett.*, *33*(12), 1010–1011.

Basu, S., K. M. Groves, J. M. Quinn, and P. Doherty (1999), A comparison of TEC fluctuations and scintillations at Ascension Island, *J. Atmos. Sol. Terr. Phys.*, *61*, 1219–1226.

Basu, Su., and S. Basu (1985), Equatorial scintillations: Advances since ISEA-6, *J. Atmos. Terr. Phys.*, *47*, 753–768.

Basu, Su., et al. (2005), Two components of ionospheric plasma structuring at midlatitudes observed during the large magnetic storm of October 30, 2003, *Geophys. Res. Lett.*, *32*, L12S06, doi:10.1029/2004GL021669.

Bhar, J. N., A. DasGupta, and S. Basu (1970), Studies on *F*-region irregularities at low latitude from scintillation of satellite signals, *Radio Sci.*, *5*, 939–942.

DasGupta, A., S. Basu, J. Aarons, J. A. Klobuchar, and A. Bushby (1983), VHF amplitude scintillations and associated electron content depletions as observed at Arequipa, Peru, *J. Atmos. Terr. Phys.*, *45*, 15–26.

DasGupta, A., S. Ray, A. Paul, P. Banerjee, and A. Bose (2004a), Errors in position-fixing by GPS in an environment of strong equatorial scintillations in the Indian zone, *Radio Sci.*, *39*, RS1S30, doi:10.1029/2002RS002822.

DasGupta, A., S. Ray, and P. Banerjee (2004b), Northern limit of the equatorial irregularity belt in the Indian zone observed with GPS signal scintillations, paper presented at International Beacon Satellite Symposium 2004 (BSS-04), Int. Cent. Theor. Phys., Trieste, Italy.

Fejer, B. G., and M. C. Kelley (1980), Ionospheric irregularities, *Rev. Geophys.*, *18*, 401–454.

Fejer, B. G., E. Kudeki, and D. T. Farley (1985), Equatorial *F*-region zonal plasma drifts, *J. Geophys. Res.*, *90*, 12,249–12,255.

Kelley, M. C. (1989), *The Earth's Ionosphere*, 115 pp., Elsevier, New York.

Kintner, P. M., H. Kil, T. L. Bleach, and E. R. de Paula (2001), Fading timescales associated with GPS signals and potential consequences, *Radio Sci.*, *36*, 731–743.

Kintner, P. M., B. M. Ledvina, E. R. de Paula, and I. J. Kantor (2004), Size, shape, orientation, speed, and duration of GPS

equatorial anomaly scintillations, *Radio Sci.*, *39*, RS2012, doi:10.1029/2003RS002878.

Rodrigues, F. S., E. R. de Paula, M. A. Abdu, A. C. Jardim, K. N. Iyer, P. M. Kintner, and D. L. Hysell (2004), Equatorial spread *F* irregularity characteristics over São Luís, Brazil, using VHF radar and GPS scintillation techniques, *Radio Sci.*, *39*, RS1S31, doi:10.1029/2002RS002826.

Sinclair, J., and R. F. Kelleher (1969), The *F*-region equatorial irregularity belt as observed from scintillation of satellite transmission, *J. Atmos. Terr. Phys.*, *31*, 201–206.

Tsunoda, R. T. (1981), Time evolution and dynamics of equatorial backscatter plumes: 1. Growth phase, *J. Geophys. Res.*, *86*, 139–149.

Tsunoda, R. T., R. C. Livingston, J. P. McClure, and W. B. Hanson (1982), Equatorial plasma bubbles: Vertically elongated wedges from the bottomside *F* layer, *J. Geophys. Res.*, *87*, 9171–9180.

Weber, E. J., J. Buchau, and J. G. Moore (1980), Airborne studies of equatorial *F* layer ionospheric irregularities, *J. Geophys. Res.*, *85*, 4621–4641.

Woodman, R. F., and C. La Hoz (1976), Radar observations of *F* region equatorial irregularities, *J. Geophys. Res.*, *81*, 5447–5466.

Yeh, K. C., H. Soicher, and C. H. Liu (1979), Observations of equatorial ionospheric bubbles by the radio propagation method, *J. Geophys. Res.*, *84*, 6589–6594.

S. Ananthakrishnan, Tata Institute of Fundamental Research, National Center for Radio Astrophysics, Ganeshkhind, Pune, Maharashtra 411007, India.

A. Das, A. DasGupta, and S. Ray, S. K. Mitra Center for Research in Space Environment, University of Calcutta, 92 Acharya Prafulla Chandra Road, Calcutta 700009, India. (adg1bkpr@hotmail.com)

A. Paul, Institute of Radio Physics and Electronics, University of Calcutta, 92, Acharya Prafulla Chandra Road, Calcutta 700009, India.